# Studies on the Density, Distribution, and Surface Phenotype of Intraepithelial Class II Major Histocompatability Complex Antigen (Ia)-Bearing Dendritic Cells (DC) in the Conducting Airways

By Michael A. Schon-Hegrad,* Jane Oliver,* Paul G. McMenamin,‡ and Patrick G. Holt*

*From the *Division of Cell Biology, Western Australian Research Institute for Child Health, Princess Margaret Hospital, Roberts Road, Subiaco, Western Australia 6008; and the ‡Department of Anatomy and Human Biology, University of Western Australia*

## Summary

Conventional immunohistochemical analysis of airway intraepithelial class II major histocompatibility complex (Ia) expression demonstrates a morphologically heterogeneous pattern of staining, suggestive of the presence of a mixed population of endogenous antigen presenting cells. Employing a novel tissue sectioning technique in conjunction with optimal surface antigen fixation, we now demonstrate that virtually all intraepithelial Ia staining throughout the respiratory tree in the normal rat, can be accounted for by a network of cells with classical dendritic cell (DC) morphology. The density of DC varies from 600–800 per $mm^2$ epithelial surface in the large airways, to 75 per $mm^2$ in the epithelium of the small airways of the peripheral lung. All the airway DC costain for CD4, with low-moderate expression of a variety of other leukocyte surface markers. Both chronic (eosinophilic) inflammation and acute (neutrophilic) inflammation, caused respectively by inhalation of chemical irritants in dust or aerosolised bacterial lipopolysaccharide (LPS), are shown to be accompanied by increased intraepithelial DC density in the large airways (in the order of 50%) and up to threefold increased expression of activation markers, including the $\beta$ chain of CD11/18. The kinetics of the changes in the DC network in response to LPS mirrored those of the transient neutrophil influx, suggesting that airway intraepithelial DC constitute a dynamic population which is rapidly upregulated in response to local inflammation. These findings have important theoretical implications for research on T cell activation in the context of allergic and infectious diseases in the respiratory tract.

The maintenance of homeostasis in the lung requires precise control of local interactions between inhaled antigens impinging on epithelial surfaces in the airways, and the underlying cells of the respiratory mucosal immune system. In particular, an efficient mechanism is required for discrimination between pathogenic antigens such as those present on bacteria and viruses, and inert nonpathogenic antigens (pollens, animal danders, etc.) which are ubiquitous in the natural environment. The failure on the part of the T cell system to maintain this distinction appears to underly a variety of immunoinflammatory diseases in the respiratory tract (1, 2). A key element of local immune regulation in the lung is thus the nature of the cell population(s) responsible for the initial presentation of inhaled antigens to T cells. Recent studies from a number of laboratories have focused attention on the potential role of dendritic cells (DC)[1] analogous to those initially described by Steinman et al. (3), in antigen recognition in the lung. DC which exhibit strong antigen-presenting activity in vitro have been extracted from enzymatic digests of parenchymal lung tissue (4–8) and from the tracheal epithelium (9), and $Ia^+$ cells with classical dendritic morphology have been identified in tissue sections from these sites at both the light and electron microscopic level (5, 9–11).

To elucidate the role of these DC populations in regulation of T cell activation in the lung and airways, detailed information is required on their density, distribution, population dynamics, and surface phenotype. This has not previously been feasible due to the technical problems associated with accurate identification and quantitation of these cells within the various complex tissue microenvironments of the respiratory tree. However, we have recently described a new tissue sectioning technique which provides a "plan" view of cell populations within the airway epithelium, akin to that seen with epidermal sheets. Employing this procedure in preliminary studies with human (12) and rat (13) airway tissues

[1] *Abbreviations used in this paper:* BALT, bronchus-associated lymphoid tissue; DC, dentritic cell; HRP, horseradish peroxidase; RT, room temperature; SHAM, sheep anti-mouse.

 J. Exp. Med. © The Rockefeller University Press • 0022-1007/91/06/1345/12 $2.00
Volume 173 June 1991 1345–1356

we have demonstrated the presence of a much denser network of intraepithelial DC than has previously been recognized. In the present study, we have used this technique to provide quantitative data on the population density, distribution, and surface phenotype of airway intraepithelial DC in normal and inflamed airway tissue.

## Materials and Methods

*Animals.* Specific Pathogen Free (SPF) Wistar Furth rats and Balb/C mice were obtained from the Animal Resources Centre (Murdoch University, Perth, Western Australia) and were barrier housed. Brown Norway (BN) rats were derived from SPF stock and were housed under conventional conditions until used. Human airway tissue was obtained from histologically normal segments of lung from patients undergoing pneumonectomy for removal of localized pulmonary malignancy.

*Exposure of Rats to Airborn Irritants.* At the commencement of these studies, bedding material employed in our rat cages comprised of wood shavings derived from *Pinus radiata*. A variable proportion of animals housed in this fashion displayed evidence of patchy inflammation in the large airways. Subsequent measurement of respirable dust within these cages by methods detailed in (14) demonstrated levels between 600–850 $\mu g/M^3$ air. Airway samples from these animals were accordingly examined separately (vide infra). The majority of the caging in our animal house was changed to low-dust (<100 $\mu g/M^3$ air) autoclaved chaff, and except where specified the results presented below are from animals housed on this material.

In a separate series of experiments, groups of animals were exposed for 1 h to aerosols of Enterobacter Agglomerans LPS generated from a solution containing 200 $\mu g$/ml saline by methods detailed in reference 15. Both small (1 $\mu m$) and large droplet (3–7 $\mu m$) aerosols were employed with identical results, and are not distinguished in the text.

*Antibodies.* The mAbs W3/25 (CD 4), Ox 6 (Ia), Ox 41, and Ox 42 ($\beta$ chain of CD11/CD18) were kindly provided by Drs. A. Williams and D. Mason (Medical Research Council Cellular Immunology Unit, Oxford, UK) and have been described in detail (16, 17). The ED series of MoAbs against a series of markers on DC and other leucocytes (18, 19) were kindly provided by Drs. C. Dijkstra and G. Kraal (Department of Histology, Vrije University, Amsterdam, The Netherlands). For Ia staining in the Balb/C mouse trachea the MoAb M5/114 was used (20), and FMC 52 was employed for human airway tissue as previously described (12).

Biotinylated sheep anti-mouse IgG (SHAM) and streptavidin-horseradish peroxidase (HRP) conjugates were purchased from Amersham (Sydney, Australia).

*Tissue Sectioning and Immunostaining.* Tracheal and lung tissue was removed from the rats immediately after sacrificing with an overdose of Nembutal. The first 6–7 mm of trachea distal to the larynx was the standard tracheal tissue removed for investigation. In some experiments, rat tracheas were dissected out in combination with up to the subsequent four generations of conducting airways. These tissues were immediately fixed "en bloc" in cold (4°C) absolute ethanol for a total of 4–18 h. Initially, lungs were carefully inflated with cold absolute ethanol, and then subjected to a gentle vacuum in cold ethanol to facilitate the penetration of the fixative and the removal of all the air.

After fixation, the lungs were cut into 1 cm blocks, and the tissue samples were rehydrated through a graded series of alcohols up to PBS then placed overnight in a 1:1 PBS/OCT freezing medium mixture (Tissue Tex II; Miles Laboratories Inc., Naperville, IL) at 4°C. Lung tissue again was subjected to a gentle vacuum to ensure complete infiltration with OCT/PBS. Subsequently, the tissues were placed in freezing capsules containing OCT medium and snap frozen with liquid nitrogen cooled isopentane. The fixed frozen tissue blocks were stored at −70°C until required.

Frozen sections of airways were cut using a Bright Cryostat either in a longitudinal plane (i.e., vertically through the epithelium in approximately the center of the airway parallel to its long axis) or in a tangential plane. The latter process, described in reference 13 involves initially mounting the trachea horizontally, and then taking sequential sections tangential to the tracheal tube. The tangential sections provide patches of epithelium, effectively sectioned parallel to the underlying basement membrane perpendicular to the long axis of the epithelial cells, and appropriate intraepithelial fields can be readily identified in stained sections via the regular sheet-like appearance of the epithelial nuclei (vide infra). 10 $\mu m$ sections were routinely employed in this study. After cutting and mounting on gelatin coated slides, the sections were air-dried for 1–2 h. Before incubation with the primary antibodies, the sections were washed briefly in PBS to remove any remaining OCT.

Immunoperoxidase detection of cell surface antigens was based on a modified indirect technique described previously (21). The primary antibody incubation was carried out for 40 min at room temperature (RT) followed by three sequential 5-min washes in PBS. The sections were then incubated with biotinylated-SHAM followed by the streptavidin-HRP for 40 min each with appropriate PBS washes in between. Development of peroxidase reaction product was carried out at RT for 10–15 min in a mixture of 12 mg of 3,3 diaminobenzidine tetrahydrochloride (DAB) in 10 ml of PBS (pH 7.6) to which 5 $\mu l$ of 30% vol/vol $H_2O_2$ had been added. For weak staining antibodies, this final incubation step was carried out at 37° C, significantly enhancing the quantity of brown reaction product.

Sections incubated without primary antibody in the first step were routinely included as controls for endogenous peroxidase. Irrelevant antibodies (viz. mouse anti-human) served as additional controls in some experiments. No significant endogenous peroxidase activity was observed within the tracheal epithelium of normal healthy rats. The sections were routinely counterstained in hematoxylin.

*Quantitation of DC Populations.* For the purposes of this study, DCs visible in tangential epithelial patches were defined on the basis of classical dendritic (Langerhans Cell-like) morphology in association with surface staining for Ia antigen. Similar morphological criteria were applied to the other surface markers.

DC density per $mm^2$ tracheal epithelium was determined by counting stained tangential sections, with the aid of a calibrated graticule. A minimum of 200 DC were counted for each tracheal sample.

To provide an estimate of DC density in successive airway generations below the trachea, where the small size mitigated against controlled tangential sectioning, the following procedure was devised. Firstly, tracheal sections from the series described in Table 1 were rescanned to identify regions where the plane of section was approximately longitudinal and thus transverse through the epithelium, i.e., analogous to that shown in Fig. 1 *A*. This provides a clear view of the line of demarcation between the basement membrane and the epithelium, and above the latter the airway lumen. Regions of longitudinally sectioned epithelium are routinely found in these mounts in similar (or greater) frequency to adjacent tangential sections, due to the irregular topography of the airway wall. Previous studies have determined that the $Ia^+$ cell population visible in longitudinally sectioned airway epithelium is only one cell deep (12, 13). Also, the tangential sections (e.g. see Fig.

1 *B*) confirm that all Ia$^+$ cells in normal SPF rat trachea can be classified as DC on the basis of morphology. Thus, for each sample in the series in Table 1, randomly selected fields of longitudinally sectioned epithelium were scanned, and the number of intraepithelial Ia$^+$ cells enumerated per unit (graticule) length. A minimum of 200 Ia$^+$ cells were counted for each sample. By relating this figure for each animal to the individual count of DC per mm$^2$ visible in plan view (i.e., tangential section) in the same tissue sample, ratios were obtained to convert numbers of Ia$^+$ cells per unit graticule length of longitudinally sectioned epithelium to DC density per mm$^2$ epithelium. This ratio was subsequently applied to figures obtained from stained longitudinal sections of airway generations 1–4 in SPF rats; initial preparation of the latter was carried out by dissection distal to the trachea, and they were then fixed as above and sectioned longitudinally. For generations $\geq 5$, random sections of peripheral lung were examined, and small longitudinal airway epithelium segments were selected for counting and data from these were pooled.

## Results

*Importance of Plane of Tissue Section and Fixation Conditions in Demonstration of the Intraepithelial DC Network.* Fig. 1 illustrates a series of frozen sections of rat trachea, stained by immunoperoxidase for Ia with the MoAb Ox6. The plane of section in Fig. 1 *A* is vertical through the airway epithelium, i.e., perpendicular to the underlying basement membrane, and shows a staining pattern typical of longitudinal or transverse sections. Ia$^+$ cells appear both within and below the epithelium. A stained cell with spindle shaped morphology (candidate DC) is highlighted within the epithelium. However, adjacent intraepithelial Ia$^+$ cells are of indeterminate morphology.

Fig. 1 *B* displays the Ia staining pattern when the trachea is sectioned tangential to the long axis of the tube and hence parallel to the epithelial basement membrane. The Ia$^+$ cells now appear in plan view against a background of counterstained epithelial nuclei, and are revealed as a highly developed intraepithelial network comprising exclusively dendritic-shaped cells. Control sections (not shown) stained for endogenous peroxidase showed no reaction product within the epithelium.

In Fig. 1 *C* the plane of section was identical to Fig. 1 *B*, but ethanol fixation was carried out after (rather than before) tissue sectioning. While numerous Ia$^+$ cells are again visible within the epithelium, much of the staining on the fine dendritic processes characteristic of these cells is lost, and the overall picture is now of a mixed Ia$^+$ mononuclear population which could logically be classified as predominantly macrophages/monocytes plus occasional DC. In our hands, cold ethanol fixation before freezing and cutting the tissue as described has provided superior antigen preservation compared to cold acetone, ethanol or methanol fixation carried out after cutting fresh frozen sections. The "en bloc" fixation described preserves dendritic structure optimally, presumably by preventing loss or diffusion of surface antigens which may occur during freezing of fresh tissue and subsequent thawing before fixation, as in the standard protocols.

*Interspecies Comparison.* Fig. 2 illustrates Ia$^+$ intraepithelial DC in tangential airway sections from rats (Fig. 2 *A*), compared to mice (Fig. 2 *B*) and human (Fig. 2 *C*). In all three species these DC display comparable morphology in relation to shape of the cell body and pattern of branching of cytoplasmic processes. High levels of Ia staining are seen over the surface of the cell bodies and along the prominent cytoplasmic processes.

*Distribution and Density of Airway Intraepithelial DC in the Steady State.* The experiments in Table 1 examine variations in DC density within the tracheal epithelium of a group of age and sex-matched SPF Wistar Furth rats. The data indicate consistent differences between the dorsal and ventral surfaces of the trachea, which are likely to reflect increased local vascularity associated with the underlying trachealis muscularis; comparable differences in local cellularity within rat tracheal epithelium have previously been noted for mast cells (22). Similarly figures for DC density were obtained with BN rats (data not shown).

In Fig. 3, intraepithelial DC density is illustrated at different levels of the respiratory tree, and a sharp decrease in density was observed after the third airway generation.

*Additional Sources of Intraepithelial Ia Staining.* In SPF rats which are free of infection and which do not display any evidence of inflammation in the airways, the only intraepithelial Ia staining we have observed which is not attributable to DC-like cells occurs above mucosal lymphoid aggregates (bronchus-associated lymphoid tissue [BALT]). Fig. 4 *A* illustrates a BALT-like aggregate below the ciliated bronchial epithelium from a normal SPF rat, shown in vertical section. Strong Ia staining was evident within the BALT itself, and the epithelial cells directly above also stain positively–adjacent respiratory (ciliated) epithelial cells are Ia$^-$.

The tangential airway epithelial section illustrated in Fig. 4 *B* contains a mixed population of heavily stained cells, comprising Ia$^+$ DC which display typical dendritic morphology comparable to those in Fig. 1 *B*, plus an infiltrate of smaller regular shaped endogenous-peroxidase positive granulocytes

**Table 1.** *Intersite and Interanimal Variation in Tracheal Epithelial Dendritic Cell (DC) Density*

| Rat no.* | Ventral | Dorsal |
|---|---|---|
| 1 | 737 | 1034 |
| 2 | 861 | 974 |
| 3 | 720 | 893 |
| 4 | 696 | 910 |
| 5 | 532 | 808 |
| 6 | 630 | 764 |
| 7 | 553 | 782 |
| | 675 ± 114‡ | 881 ± 101 |

* Age matched Wistar Furth adult females.
‡ $\bar{X}$ ± S.D.
Dorsal>ventral: $p < 0.0005$ by paired t-test.

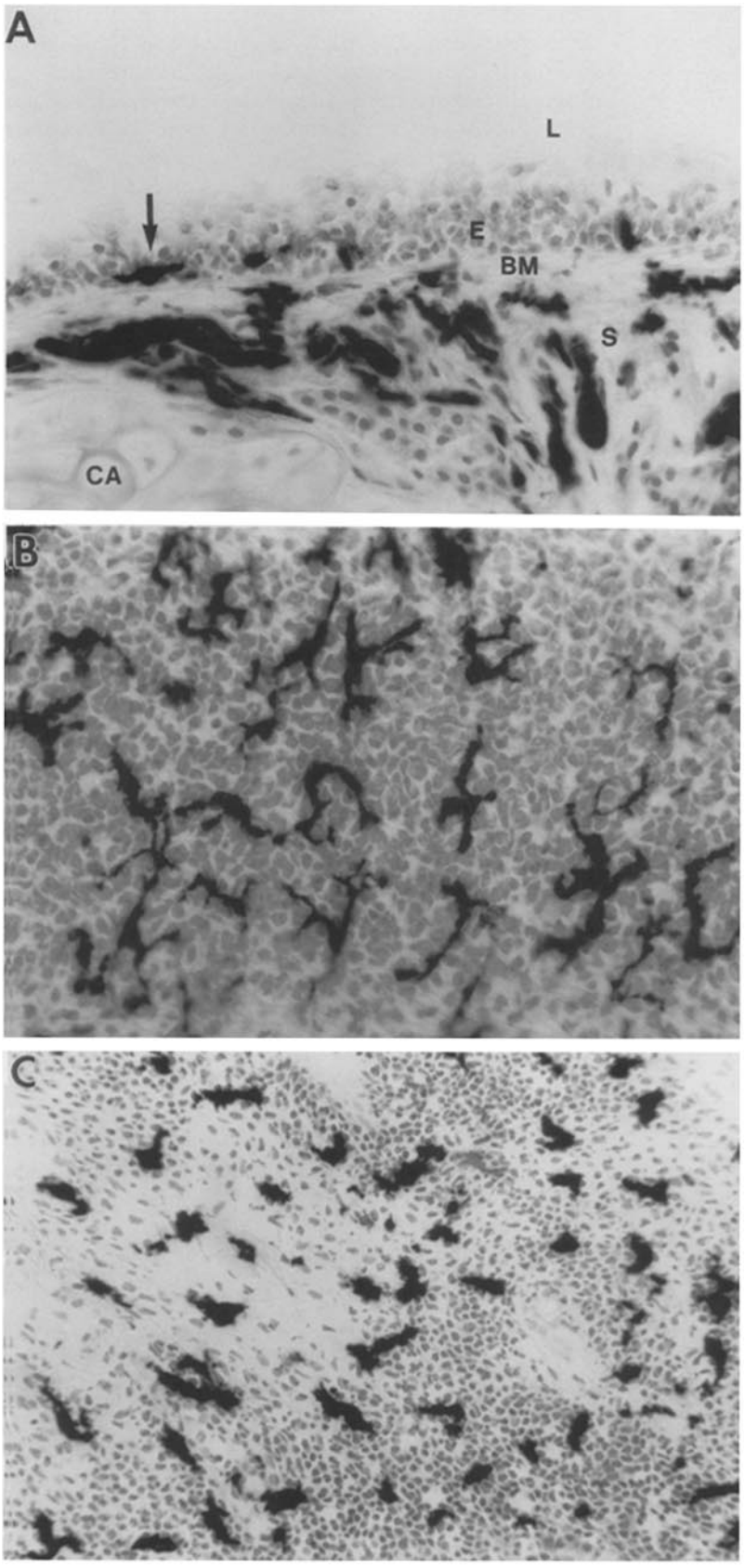


**Figure 1.** Ia immunostaining patterns in normal rat tracheal epithelium. Frozen segments of Wistar Furth strain rat trachea were sectioned longitudinally (*A*) or tangentially (*B* and *C*) and immunostained for Ia as detailed in the text, employing the MoAb Ox6. A control mouse antibody gave no staining within the epithelium, but occasional endogenous-peroxidase positive cells were observed in the submucosa. (→) Candidate DC; (L) airway lumen; (E) epithelium; (BM) basement membrane; (S) submucosa; (CA) cartilage. (*A* and *B*, obj. 40×; *C*, obj. 25×).

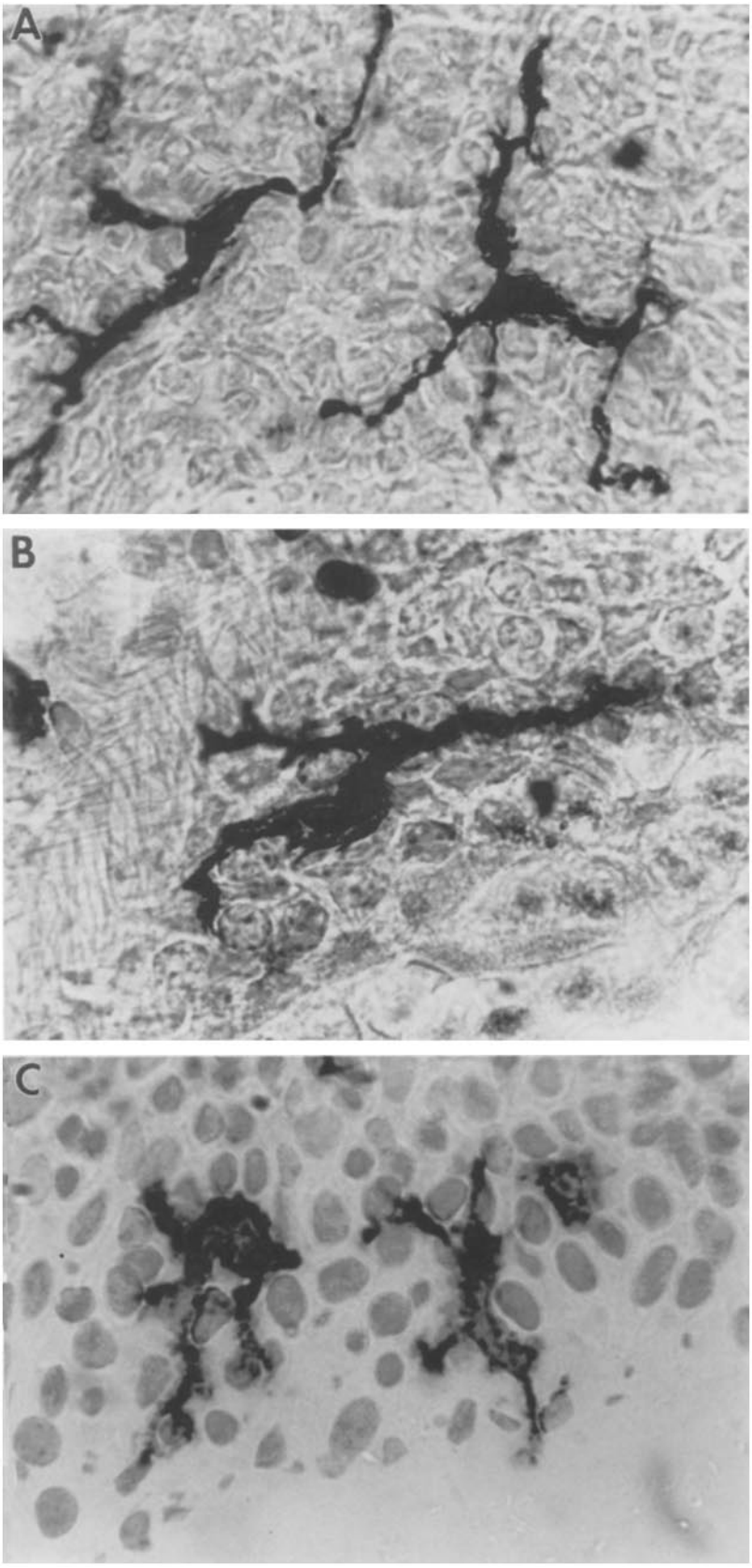


**Figure 2.** Ia$^+$ DC in airway epithelium of different species. Frozen tangential sections of rat trachea (*A*), mouse trachea (*B*), and human bronchiole (*C*) immunostained for Ia. (obj. 100×).

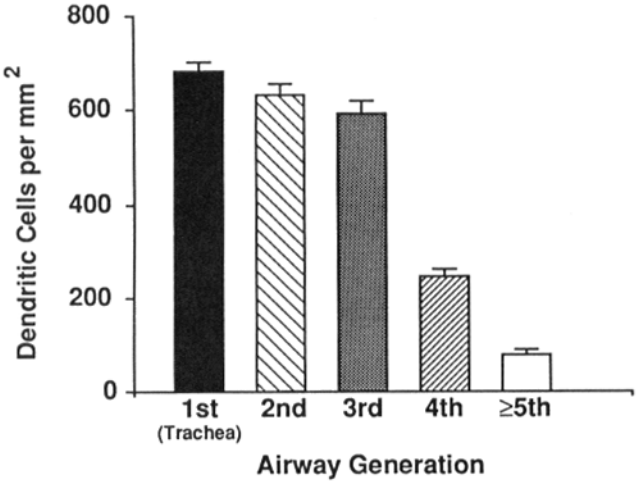


**Figure 3.** DC density in the conducting airways of inflammation-free SPF Wistar Furth rats. Data shown are numbers of Ia+ cells with DC morphology per mm² epithelium, determined as detailed in the text.

(arrowed) which are indicative of local inflammation. Such infiltrates were observed within the airway epithelium (often as discrete foci) in a proportion of our barrier-housed SPF-derived rats during the initial phase of this study, and were subsequently found to be due to the use of excessively dusty *Pinus radiata* wood shaving as bedding in the cages (see Discussion below). Foci of epithelial Ia staining were often observed in association with such granulocytic infiltrates, of which Fig. 4 *B* is a typical example.

*Intraepithelial DC in Chronically Inflamed Airways.* The observation of these zones of focal airway inflammation early in this study prompted the change to low-dust autoclaved chaff bedding, and "normal" data are derived from animals raised on the latter. However, airway samples from the rats housed on *Pinus radiata* woodshavings were used to provide initial information on the effects of inflammation on the airway DC network.

Thus in the experiments in Table 2, areas of normal epithelium (analogous to Fig. 1 *B*) were directly compared to inflamed epithelium (analogous to Fig. 4 *B*) from the animals housed on wood shavings. The mean density of intraepithelial DC was significantly increased in the inflamed tissue (Table 2), and their dendritic processes superficially appear thicker and more branched than those on DC in the normal tissue samples. We are unable at present to determine whether the increased deposition of peroxidase reaction product overlying the dendrites from these cells is associated with thickening of the processes per se or with increased expression of surface Ia. However, it is clear that net expression of certain other surface markers on the DC population is increased at inflammatory foci. A typical example is shown in Fig. 5 *B* which illustrates intense staining of DC-like cells with the MoAb Ox42 together with numerous smaller granulocytes within a localized region of tracheal epithelial inflammation (left half of photomicrograph), adjacent to an area of normal epithelium (right half of micrograph) containing few Ox42-stained cells.

A quantitative analysis of these differences in intraepithelial staining patterns using a panel of MoAb, is shown in Table 3.

None of the MoAbs currently available for immunostaining of DC and inflammatory cells in the rat are lineage-specific. However, the use of dendritic morphology in conjunction with constitutive high expression of Ia (17, 19, 23) provides an acceptable reference point for this type of analysis. Thus in the published studies listed in the top section of Table 3 the frequency of Ia+ (Ox6+) cells with DC-like morphology was set at 100 for each organ, and the data for staining of cells (with comparable morphology) with the other MoAbs was normalized accordingly.

The table also shows relative staining frequencies for inflammatory cells. It can be seen that considerable overlap exists between macrophages and DC populations in this species and it could be argued that morphological criteria alone are too subjective to permit consistently accurate discrimination between these cell types. However, differential staining with the Ox6 (anti-Ia) and the ED series of mAbs (particularly ED8 which stains all monocytes, macrophages, and granulocytes) provides additional objective criteria for discrimination, and in some tissue microenvironments major differences are also evident in staining with W3/25 (anti-CD4) and Ox42 (anti-B chain of CD11/18). Granulocytes are readily distinguishable in tissue sections by size and morphology, and may be subdivided into eosinophils and neutrophils on the basis of endogenous peroxidase staining (eosinophils stain heavily while neutrophils are negative; data not shown).

In the experiments illustrated at the bottom of Table 3, this panel of MoAbs was employed to stain airway tissues from these animals. DC-like cells from normal tissue demonstrated low reactivity with the ED9 and Ox41/42 MoAbs, and chronic inflammation was associated with marked increases in expression of these markers. The infiltrate of small round cells in the inflamed tissues (see Fig. 4 *B*) stained very strongly for endogenous peroxidase, which indicates they are

**Table 2.** *Effect of Chronic Inflammation on Dendritic Cell (DC) Density in Tracheal Epithelium*

| Rat no.* | Noninflamed | Rat no. | Inflamed‡ |
|---|---|---|---|
| 1 | 643 | 6 | 726 |
| 2 | 502 | 7 | 584 |
| 3 | 566 | 8 | 785 |
| 4 | 516 | 9 | 664 |
| 5 | 556 | 10 | 829 |
| | 557 ± 55§ | | 718 ± 97 |

* Animals were age-matched BN adult females.
‡ Nonspecific inflammation characterized by patches of Ia+ epithelium and infiltrates of endogenous peroxidase positive granulocytes (eosinophils).
§ $\bar{X}$ ± S.D.
Inflamed > noninflamed: $p < 0.05$ by t-test.

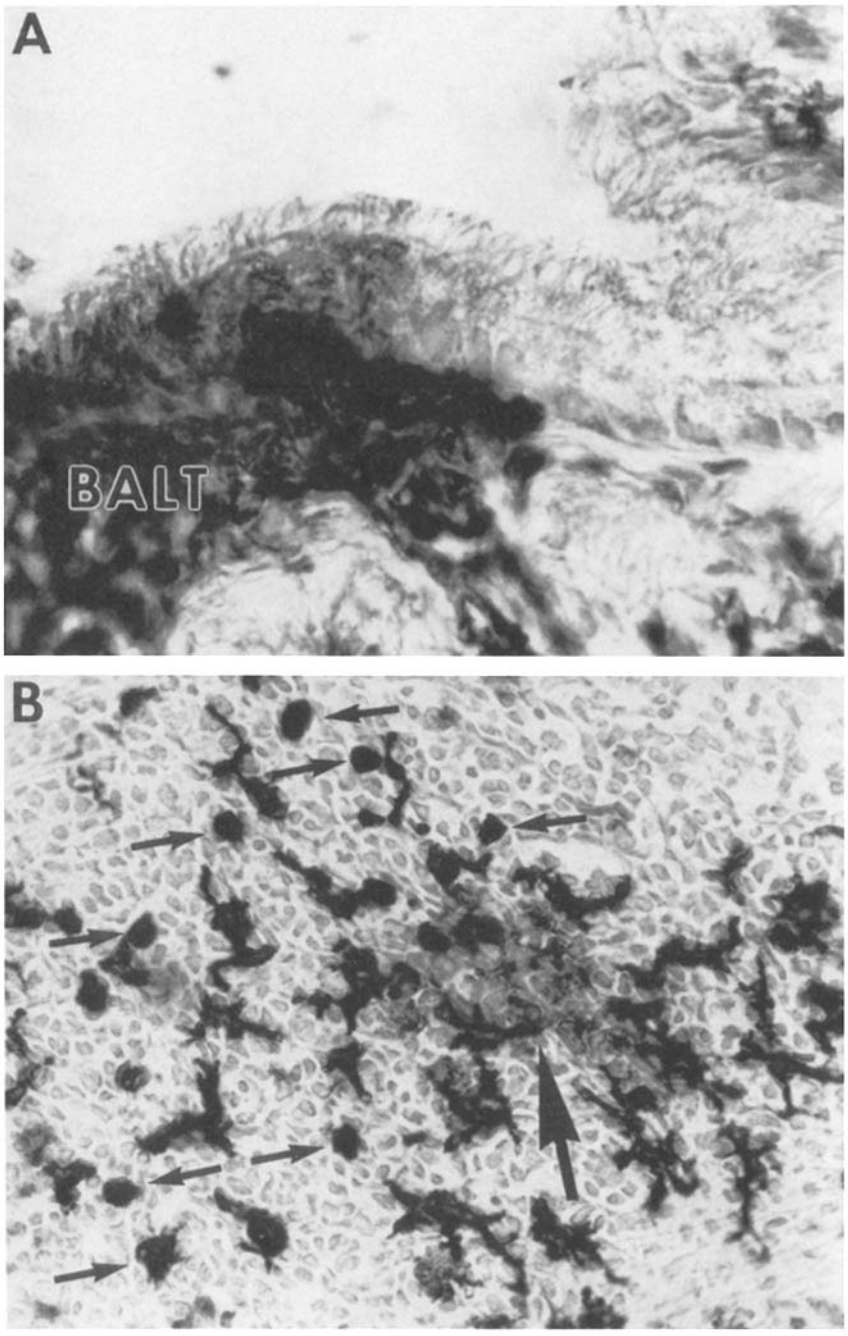


**Figure 4.** Expression of Ia in rat airway epithelial cells. Frozen longitudinal section of normal BN bronchus showing BALT (*A*) and tangential section of inflamed trachea (*B*) immunostained for Ia. The donor animal in *B* was housed on *Pinus radiata* woodshavings. (→) endogenous-peroxidase positive granulocytes. (⇒) focal zone of epithelial Ia staining. (*A*, obj. 100×; *B*, obj. 40×).

eosinophils. It should be noted that these experiments do not discriminate between increased expression of surface markers on resident DC versus the influx of fresh marker-positive DC, and this issue will be addressed in subsequent studies.

*Airway Intraepithelial DC in Acute Inflammation.* In the experiments summarized in Fig. 6, groups of Wistar Furth rats were exposed to aerosols of saline or LPS in saline for a 1-h period, and sacrificed in groups of four at the time points shown. Saline exposed animals did not differ throughout the experiment and data from these animals are grouped with the zero time controls. In the bottom panel of Fig. 6 it can be seen that the density of intraepithelial DC increases by 50% at 24 h post LPS exposure, and declines to approximately normal levels by 48 h. The epithelium at the 8- and 24-h time points contained a large infitrate of small, regularly shaped cells which had disappeared by 48 h; these small cells stained strongly for Ox42, but were endogenous peroxidase negative (not shown), a pattern which is typical of neutrophils in this species. Consistent with this suggestion, parallel tissue sections stained with Giemsa revealed the presence of a similar density of small round cells with characteristic multi-lobed nuclei; occasional infiltrating cells with monocyte-like nuclei were also observed, but subsequent staining of tracheal sections from the same animals with the pan macro-

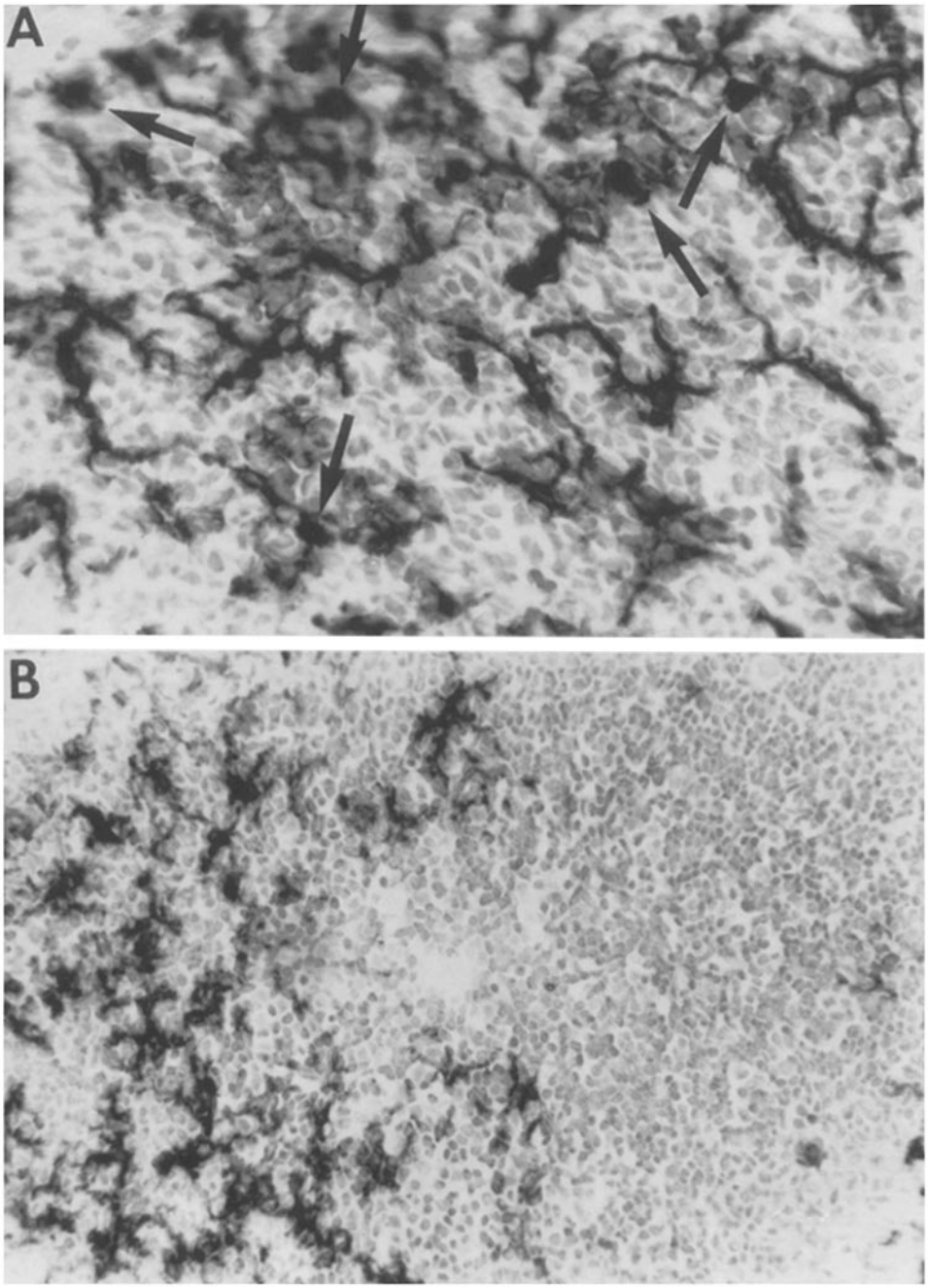


**Figure 5.** Focal inflammation in rat trachea. (*A*) High power adjacent field of inflamed epithelium from BN rat immunostained for Ia. (obj. 40×). (*B*) Tangential section of BN tracheal epithelium from the same area immunostained for Ox42. Area of focal inflammation (*left*) showing high density of Ox42$^+$ cells in conjunction with infiltrate of small Ox42$^+$ endogenous peroxidase positive granulocytes (not visible at this magnification), adjacent to normal noninflamed epithelium (*right*) showing low levels of Ox42 staining. (obj. 25×). (→) endogenous peroxidase positive granulocytes.

phages/monocyte MoAb ED1 revealed very few positive cells of this size, confirming that the infiltrate was predominantly neutrophilic. Patchy Ia staining on epithelial cells was also observed at the 24 h time point, which was similar (albeit less intense) to Fig. 4 *B*.

The top panel of Fig. 6 illustrates staining patterns in airway epithelium from control versus LPS-exposed rats at the peak of the inflammatory response (24 h). It is clear that the increase in density of the DCs is accompanied by a net increase in surface expression of markers identified by the MoAbs Ox41 and Ox42. In addition to the individual MoAbs, parallel sections were stained with a mixture of Ox6 plus either or both the other antibodies; the number of DC per mm$^2$ observed in Ox6-stained sections was not significantly different to the combinations (data not shown), indicating that the Ox41$^+$ and Ox42$^+$ DC represent a subset of the overall OX6$^+$ DC population. However, as noted above the relative contribution of resident versus recruited DC to this increased marker expression remains to be determined.

## Discussion

Previous studies from our laboratory suggest an important role for DC in regulation of T cell responses in the rat

**Table 3.** *Characterization of Airway Intraepithelial Dendritic Cell (DC) Employing a Panel of MoAbs*

| MoAb → | Ox6 | Ox41 | Ox42 | W3/25 | ED1 | ED8 | ED9 |
|---|---|---|---|---|---|---|---|
| Target Antigen → | Ia | 120-kD surface protein | B chain CD11/CD18 Family | CD4 | ND | Component of CD11/18 (≠Ox42)[§] | ND |
| Dendritic cells | | | | | | | |
| TDL | 100[*] | 50[‡] | 50[‡] | 55[‡] | – | – | – |
| Spleen/lymph node | 100[‡§] | Few[‡] | Majority[‡] | – | 90[§] | 50[§] | 50–91[§] |
| Thymic cortex | Majority[‡] | Some[‡] | Some[‡] | – | – | 0 | Majority[§] |
| Langerhans Cells | 100[‡‖] | Majority[‡] | Majority[‡] | 0[‡] | – | <10[%] | Majority[§] |
| Inflammatory cells | | | | | | | |
| Resident PM[¶] | <10[‖] | 76[‡] | 83[‡‖] | 68[‡] | 100[§‖] | 100[§‖] | 100[§] |
| Exudate PM[¶] | 15–60[‖] | 90[‡‖] | 98[‡‖] | 77[‡] | 100[§‖] | 100[§‖] | 100[§] |
| Granulocytes | 0[‖] | 70[‡‖] | 98[‡‖] | 0 | – | 100[§‖] | – |
| **Airway epithelial DC** | | | | | | | |
| **Normal** | **100** | **43** | **25** | **95** | **65** | **16** | **15** |
| **Chronic inflammation** | **100** | **95** | **84** | **–** | **–** | **30** | **77** |

Data for airway epithelial DC in inflamed versus noninflamed animals were derived from two groups of BN rats as detailed in Table 2; staining frequencies for the airway DC were normalized against figures obtained with Ox6 (anti-Ia), as per the background publications cited for other tissues.
[*] Reference (23); [‡] Reference (17); [§] Reference (19).
[‖] Verified in experiments performed here; [¶] as % peritoneal macrophages (PM).

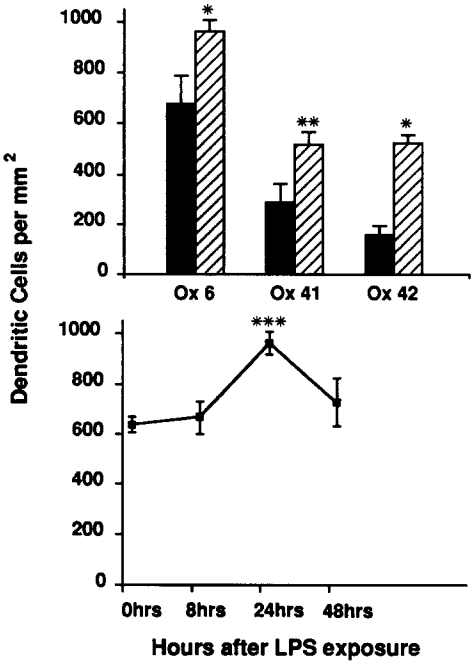


**Figure 6.** Effect of acute inflammation in response to LPS inhalation on the airway intraepithelial DC network. The upper panel illustrates densities of DC stained by the MoAbs listed, in tracheal epithelial samples from normal Wistar Furth rats (■) and age-matched animals 24 h after exposure to an aerosol of LPS (▨). Data shown are $\bar{X} \pm SD$ derived from four animals per group. The lower panel shows frequencies of Ia$^+$ cells with DC-like morphology, as a function of hours post LPS aerosol exposure. Ox42 staining at 48 h was also markedly reduced relative to 24 h (not shown). LPS > control: $^*p < 0.00005$; $^{**}p < 0.005$; $^{***}p < 0.0005$ by t-test.

respiratory tract. In this species DC appear to be the only resident cell present in noninflamed alveolar septa (4) or airway epithelium (9) which are capable of presenting antigen-specific activation signals to immune T cells in vitro. Moreover, we have established that enriched populations of DC prepared from the tracheal epithelium of rats following exposure to an aerosol containing ovalbumin are capable of stimulating the proliferation of OVA-immune T cells in culture, which indicates that the airway epithelial DC population are capable of trapping inhaled antigen in situ (9).

The present study confirms that this DC network constitutes the sole source of Ia$^+$ cells within the normal intact epithelium, which reinforces the view that they serve as the first line of defense against incoming antigen, and as such must be intimately involved in the pathogenesis of infectious and allergic diseases in the airways. Their acknowledged role as the major stimuli for induction of MLR reactions (24) also stamps them as prime candidates for initiation of graft rejection reactions in lung transplant recipients, where the focus of immunological injury is in the airways (25, 26).

This airway intraepithelial DC network thus represents

a potentially important therapeutic target in a range of important respiratory diseases. However, detailed information on the distribution, population dynamics, and surface phenotype(s) of the cells which form the network represent minimal prerequisites for such applied research, and the present study provides the first such data in a defined animal model.

The salient findings from this study are as follows. First, the epithelium lining the conducting airways in all species examined contains a highly developed network of DC-like cells which closely resemble the Langerhans cell population in the epidermis. The DC densities found in rat tracheal epithelium (Table 1) are comparable to published data for skin and oral mucosa in mouse, guinea pig, hamster, and rat (27, 28), and are considerably higher than those reported for immunologically privileged sites (27). As shown in Fig. 1, the demonstration of the airway intraepithelial DC network requires rigorous control of both sectioning plane and fixation methodology, in particular the former, as the classical dendritic morphology of these cells is inapparent in conventional transverse or longitudinal airway sections.

Second, despite the lack of a MoAb specific for DC, the identification of these cells in immunostained tangential airway epithelial sections from normal animals can be achieved satisfactorily via the use of a MoAb against Ia in conjunction with a panel of antibodies against a range of other cell surface markers, including some which are panspecific for macrophages. Thus it is evident that virtually all of the airway epithelial DC express CD4 in the steady state (Table 3), which contrasts with lymph born DC in this species where CD4 staining is restricted to 55% of the population (17) and Langerhans cells which have been reported as $CD4^-$ (15). All rat macrophages/monocytes express both CD4 (16, 17) and the marker ED1 (18); the latter is also expressed on some DC-like cells in a variety of lymphoid tissues (18), and is found on up to 65% of airway intraepithelial DC (Table 3). The MoAbs Ox41 and Ox42 stain 50% of rat lymph born DC and approximately 90% of macrophages (17), and in our hands identify respectively 43% and 25% of DC in the airway epithelium (Table 3). Antibodies ED8 and ED9 react with 100% of resting and activated macrophages in the blood and the peritoneal cavity (19), but stain only a small proportion of normal airway epithelial DC (Table 3). It is noteworthy that DC in alveolar septal walls fail to stain with the ED1 MoAb (10), which emphasizes the importance of local tissue-derived factors in modulation of DC maturation within different microenvironments in the lung. Similar conclusions follow from the use of the MoAb ED2 (16) which stains the majority of alveolar DC (10), but does not react with any of their counterparts in the epithelium of the conducting airways (data not shown). We have additionally noted that large ED2 positive DC-like cells are also found on the submucosal side of the epithelial basement membrane (comparable to the population of $Ia^+$ cells in the submucosa in Fig. 1 *A*), and experiments are in progress to phenotype this population.

This study also provides the first direct evidence that airway intraepithelial DC populations change both quantitatively and qualitatively during inflammation. The initial observations in this context noted the presence of prominent eosinophilic infiltrates in tracheal epithelial sections from animals which had been housed on pine woodshavings (Fig. 5 *A*). Subsequent investigations demonstrated high levels of airborne respirable pine dust within the animals' cages, and this agent has previously been shown to cause direct cytotoxic damage to rat tracheal epithelium via the action of abietic acids present in the pine resin (29). The eosinophilia observed in these sections is consistent with chronic inflammation, which in our animals was accompanied by a mean increase of 28% in intraepithelial DC density (Table 2) as well as increased expression of a variety of markers on the surface of the DCs (bottom of Table 3). Noteably, the DC population demonstrate > three-fold increased staining with the MoAb Ox42 which reacts with the common $\beta$ chain of the CD11/18 family of cell adhesion molecules, and it's heightened expression during inflammation may underly major functional changes in the DCs.

More compelling evidence of a role for DC in the pathogenesis of airway inflammation was provided by experiments which examined the acute response to inhaled LPS (Fig. 6). Exposure to LPS aerosols provokes a classical acute inflammatory response in the lungs, the hallmark of which is a transient influx of neutrophils into the airways which peaks between 8 and 24 h post exposure (30) followed by a later and smaller wave of monocytes/macrophages. In these experiments the epithelium of LPS-exposed rats at 24 h after LPS exposure exhibited a prominent but transient influx of small cells which were predominantly neutrophils, and in addition demonstrated a 50% increase in intraepithelial DC density. Concomitantly, net surface expression within the DC population of the $\beta$ chain of CD11/18 plus the marker stained by Ox41 also increased markedly, which collectively indicates that rapid changes in the intraepithelial DC network constitute an integral component of the acute phase of the inflammatory response in the airways. It is also noteworthy that the changes in DC density in Fig. 6 mirror the rapid kinetics of the LPS-induced acute inflammatory response in the airways (30), suggesting major alterations in the half-life of the intraepithelial DC population. This finding has important theoretical implications in relation to transport of inhaled antigens to T cells in regional lymph nodes during inflammation, particularly in relation to allergic disease wherein airway inflammation is recognized as an important "risk factor" in primary sensitization to inhalant allergens (1, 3).

It is also noteworthy in this context that the progressively decreasing density of intraepithelial DC observed below the third airway generation in normal animals (Fig. 3) is broadly consistent with known patterns of particulate deposition within the airways, which is inversely related to airway diameter (31). This suggests that stimulation by inhaled antigens and irritants even in the steady state, may play a significant role in determining the basal activity of the airway intraepithelial DC network.

This work was supported by the National Health and Medical Research Council of Australia.

Address correspondence to Dr. Patrick G. Holt, Western Australian Research Institute for Child Health, Princess Margaret Hospital for Children, Perth Western Australia, Box D 184, GPO Perth 6001, Australia.

*Received for publication 26 September 1990 and in revised form 21 February 1991.*

## References


1. Holt, P.G., and C. McMenamin. 1989. Defence against allergic sensitization in the healthy lung: the role of inhalation tolerance. *Clin. Exp. Allergy.* 19:255.
2. Holt, P.G., C. McMenamin, M.A. Schon-Hegrad, D. Strickland, D. Nelson, L. Wilkes, N. Bilyk, J. Oliver, B.J. Holt, and P.G. McMenamin. 1990. Immunoregulation of asthma: control of T-lymphocyte activation in the respiratory tract. *Eur. Respir. J.* In press.
3. Steinman, R.M., and M.C. Nussenweig. 1980. Dendritic cells: features and functions. *Immunol. Rev.* 53:127.
4. Holt, P.G., A. Degebrodt, C. O'Leary, K. Krska, and T. Plozza. 1985. T cell activation by antigen-presenting cells from lung tissue digests: suppression by endogenous macrophages. *Clin. Exp. Immunol.* 62:586.
5. Sertl, K., T. Takemura, E. Tschachler, V.J. Ferrans, M.A. Kaliner, and E.M. Shevach. 1986. Dendritic cells with antigen-presenting capability reside in airway epithelium, lung parenchyma, and visceral pleura. *J. Exp. Med.* 163:436.
6. Nicod, L.P., M.F. Lipscomb, J.C. Weissler, C.R. Lyons, J. Albertson, and G.B. Toews. 1987. Mononuclear cells in human lung parenchyma. Characterization of a potent accessory cell not obtained by bronchoalveolar lavage. *Am. Rev. Respir. Dis.* 136:818.
7. Rochester, C.L., E.M. Goodell, J.K. Stoltenberg, and W.E. Bowers. 1988. Dendritic cells from rat lung are potent accessory cells. *Am. Rev. Respir. Dis.* 138:121.
8. Kradin, R.L., K.M. McCarthy, J. Gifford, and E.E. Schneeberger. 1989. Antigen-independent binding of T-cells by dendritic cells and alveolar macrophages in the rat. *Am. Rev. Respir. Dis.* 139:207.
9. Holt, P.G., M.A. Schon-Hegrad, and J. Oliver. 1988. MHC class II antigen-bearing dendritic cells in pulmonary tissues of the rat. Regulation of antigen presentation activity by endogenous macrophage populations. *J. Exp. Med.* 167:262.
10. Holt, P.G., and M.A. Schon-Hegrad. 1987. Localization of T cells, macrophages and dendritic cells in rat respiratory tract tissue: implications for immune function studies. *Immunology.* 62:349.
11. Soler, P., S. Chollet, C. Jacque, Y. Fukuda, V.J. Ferrans, and F. Basset. 1985. Immunocytochemical characterization of pulmonary histiocytosis X cells in lung biopsies. *Am. J. Pathol.* 118:439.
12. Holt, P.G., M.A. Schon-Hegrad, M.J. Phillips, and P.G. McMenamin. 1989. Ia-positive dendritic cells form a tightly meshed network within the human airway epithelium. *Clin. Exp. Allergy.* 19:597.
13. Holt, P.G., M.A. Schon-Hegrad, J. Oliver, B.J. Holt, and P.G. McMenamin. 1990. A contiguous network of dendritic antigen-presenting cells within the respiratory epithelium. *Int. Arch. Allergy Appl. Immunol.* 91:155.
14. Stewart, G.A., and P.G. Holt. 1985. Submicronic airbone allergens. *Med. J. Aust.* 143:426.
15. Holt, P.G., M. Reid, J. Sedgwick, and H. Bazin. 1987. Suppression of IgE responses by passive antigen inhalation: Dissociation of local (mucosal) and systemic immunity. *Cell. Immunol.* 104:434.
16. Mason, D.W., R.P. Arthur, M.J. Dallman, J.R. Green, G.P. Spickett, and M.L. Thomas. 1983. Functions of rat T-lymphocyte subsets isolated by means of monoclonal antibodies. *Immunol. Rev.* 74:57.
17. Robinson, A.P., T.M. White, and D.W. Mason. 1986. Macrophage heterogeneity in the rat as delineated by two monoclonal antibodies MRC OX-41 and MRC OX-42, the latter recognizing complement receptor type 3. *Immunology.* 57:239.
18. Dijkstra, C.D., E.A. Dopp, P. Joling, and G. Kraal. 1985. The heterogeneity of mononuclear phagocytes in lymphoid organs: distinct macrophage subpopulations in the rat recognized by monoclonal antibodies ED1, ED2, and ED3. *Immunology.* 54:589.
19. Damoiseaux, J.G., E.A. Dopp, J.J. Neefjes, R.H. Beelen, and C.D. Dijkstra. 1989. Heterogeneity of macrophages in the rat evidenced by variability in determinants: two new anti-rat macrophage antibodies against a heterodimer of 160 and 95 kd (CD11/CD18). *J. Leukocyte Biol.* 46:556.
20. Bhattaharya, A., M.E. Dorf, and T.A. Springer. 1981. A shared alloantigenic determinant on Ia antigens encoded by the I-A and I-E subregions: evidence for I region gene duplication. *J. Immunol.* 127:2488.
21. Barclay, A.N. 1981. Different reticular elements in rat lymphoid tissue identified by localization of Ia, Thy-1 and MRC OX-2 antigens. *Immunology.* 44:727.
22. Tam, E.K., L.D. Calonico, J.A. Nadel, and D.M. McDonald. 1988. Globule leukocytes and mast cells in the rat trachea: their number, distribution, and response to compound 48/80 and dexamethasone. *Anat. Embryol.* 178:107.
23. Mayrhofer, G., Holt, P.G., and Papadimitriou, J.M. 1986. Functional characteristics of the veiled cells in afferent lymph from the rat intestine. *Immunol.* 58:379.
24. Steinman, R.M., and M.D. Witmer. 1978. Lymphoid dendritic cells are potent stimulators of the primary mixed leukocyte reaction in mice. *Proc. Natl. Acad. Sci. USA.* 75:5132.
25. Griffith, B.P., I.L. Paradis, A. Zeevi, H. Rabinowich, S.A. Yousem, R.J. Duquesnoy, J.H. Dauber, and R.L. Hardesty. 1988. Immunologically mediated disease of the airways after pulmonary transplantation. *Ann. Surg.* 208:371.
26. Tazelaar, H.D., and S.A. Yousem. 1988. The pathology of combined heart-lung transplantation: an autopsy study. *Hum. Pathol.* 19:1403.
27. Bergstresser, P.R., C.R. Fletcher, and J.W. Streilein. 1980. Surface densities of Langerhans cells in relation to rodent epidermal

sites with special immunologic properties. *J. Invest. Dermatol.* 74:77.
28. Ahlfors, E.E., P.A. Larsson, and P.R. Bergstresser. 1985. Langerhans cell surface densities in rat oral mucosa and human buccal mucosa. *J. Oral. Pathol.* 14:390.
29. Ayars, G.H., Altman, L.C., Frazier, C.E., and E.Y. Chi. 1989. The toxicity of constituents of cedar and pine woods to pulmonary epithelium. *J. Allergy Clin. Immunol.* 83:610.
30. Venaille, T., Snella, M.C., Holt, P.G., and Rylander, R. 1989. Cell recruitment into lung wall and airways of conventional and pathogen-free guinea pigs after inhalation of endotoxin. *Amer. Rev. Respir. Dis.* 139:1356.
31. Phalen, R.F. 1984. In Inhalation Studies: Foundations and Techniques, CRC Press Inc., Boca Raton, Florida. pp 61–65.